Carbohydrate Polymers 92 (2013) 77–83

Contents lists available at SciVerse ScienceDirect

Carbohydrate Polymers

journal homepage: www.elsevier.com/locate/carbpol

Preparation of cellulose-*graft*-poly(ε-caprolactone) nanomicelles by homogeneous ROP in ionic liquid

Yanzhu Guo[a], Xiaohui Wang[a,*], Zuguang Shen[a], Xuancai Shu[a], Runcang Sun[a,b]

[a] State Key Laboratory of Pulp and Paper Engineering, South China University of Technology, Guangzhou 510640, China
[b] Institute of Biomass Chemistry and Technology, Beijing Forestry University, Beijing 100083, China

ARTICLE INFO

Article history:
Received 17 August 2012
Received in revised form
12 September 2012
Accepted 24 September 2012
Available online 2 October 2012

Keywords:
Cellulose
Poly(ε-caprolactone)
ROP
Self-assembly
Nanomicelles

ABSTRACT

Self-associating cellulose-*graft*-poly(ε-caprolactone) (cellulose-*g*-PCL) copolymers were successfully synthesized via homogeneous ring-opening polymerization (ROP) of ε-CL onto softwood dissolved pulp substrate in ionic liquid 1-N-butyl-3-methylimidazolium chloride ([Bmim]Cl). An organic catalyst N,N-dimethylamino-4-pyridine (DMAP) was compared with the traditional metal-based catalyst ($Sn(Oct)_2$) as the catalyst of the reaction, and exhibited higher catalytic activity. By controlling the cellulose:ε-CL feed ratio and reaction temperature, the molecular architecture of the copolymers can be altered, as evidenced by FT-IR, ^1H NMR, ^{13}C NMR, TGA and XRD. The self-assembly behavior of the copolymers in water was investigated and characterized using fluorescence probe, dynamic light scattering (DLS) and SEM. The results showed that the cellulose-*g*-PCL copolymers could form nanosized micelles (approximately 20–100 nm) in water, and the micelle size and critical micelle concentration (CMC) can be controlled by varying the grafting ratio of PCL. These cellulose-based nanomicelles are expected to be useful in broad application fields.

© 2012 Elsevier Ltd. All rights reserved.

1. Introduction

Recently, cellulose-based amphiphilic polymers and self-assembled nanomicelles are drawing increasing attention due to their great potential as the nanocarriers for drug/gene delivery, sensing, bioimaging, etc. (Chang, Peng, Zhang, & Pang, 2009; Chao-Hsuan et al., 2011; Hassani, Hendra, & Bouchemal, 2012; Wang & Sun, 2011; Wang et al., 2011; Wang, Guo, Li, Chen, & Sun, 2012). Similar with the traditional amphiphilic polymeric micelles, the self-assemblies based on amphiphilic cellulose are able to solubilize and encapsulate poorly soluble drugs and functional materials in their inner core. Furthermore, compared with the synthetic amphiphilic block copolymers, the natural polysaccharide-based amphiphiles have many promising properties, for example good biocompatibility, biodegradability, non-toxicity, non-immunogenic, etc. (Hassani et al., 2012). As the most abundant polysaccharide in nature, cellulose is especially desirable to be used as the precursor of polymeric amphiphiles considering the availability and economics.

Unfortunately, due to the extremely poor solubility of cellulose in most aqueous and organic solvents and the difficulty in cellulose processing, most self-associating amphiphilic cellulose derivatives can only be prepared from soluble cellulose derivatives (Dou, Jiang, Peng, Chen, & Hong, 2003; Francis, Piredda, & Winnik, 2003; Wei, Cheng, Hou, & Sun, 2008; Yan, Yuan, et al., 2009), e.g. ethyl cellulose (Kang et al., 2006; Li et al., 2008; Liu et al., 2012; Yuan, Zhang, Zou, Shen, & Ren, 2012), hydroxypropyl cellulose (Ostmark, Nystrom, & Malmstrom, 2008), hydroxyethyl cellulose (Hsieh, Van Cuong, Chen, Chen, & Yeh, 2008; Jiang, Wang, Sun, & Yang, 2011; Wan, Jiang, & Zhang, 2007), etc. However, This would, on the other hand, affect the biotoxicity, biodegradability and increase the expense of the amphiphilic products. Actually, direct hydrophobic or amphiphilic modification of cellulose substrate has been studied for a long history (Roy, Semsarilar, Guthrie, & Perrier, 2009). Many techniques, such as atom transfer radical polymerization (ATRP) (Carlmark & Malmstrom, 2003), ring-opening polymerization (ROP) (Habibi & Dufresne, 2008; Labet & Thielemans, 2011; Lonnberg, Fogelstrom, Berglund, Malmstrom, & Hult, 2008), reversible addition-fragmentation chain transfer (RAFT) polymerization (Liu, Chen, Sun, Liu, & Liu, 2010), and click chemistry (Krouit, Bras, & Belgacem, 2008) have been applied to cellulose modification in terms of surface modification on cellulose fiber or nanofibrils in a heterogeneous way.

Taking advantage of recent development in cellulose's novel dissolving systems, it is possible to prepare self-associating cellulose-based amphiphiles in homogenous solution. Yuan et al. reported the preparation of cellulose-*graft*-poly(N,N-dimethylamino-2-ethyl methacrylate) (PDMAEMA) copolymers by homogeneous ATRP in ionic liquid 1-allyl-3-methylimidazolium

* Corresponding author. Tel.: +86 20 87111861; fax: +86 20 87111861.
E-mail address: fewangxh@scut.edu.cn (X. Wang).

0144-8617/$ – see front matter © 2012 Elsevier Ltd. All rights reserved.
http://dx.doi.org/10.1016/j.carbpol.2012.09.058

chloride (Sui et al., 2008). The as-prepared copolymers were found to have similar pH- and temperature-responsive properties to PDMAEMA. Dong et al. (2008) prepared cellulose-*g*-PLA copolymers by ROP of L-lactide (LA) onto cellulose in ionic liquid [Amim]Cl. Zhou et al. prepared amphiphilic cellulose carrying long chain alkyl groups and its self-assembled micelle in the NaOH/urea homogeneous solution (Song, Zhang, Gan, Zhou, & Zhang, 2011). In our previous works, we described the grafting of long chain acyl groups onto microcrystalline cellulose backbone by homogeneous acylation in N,N-dimethylacetamide/lithium chloride (DMAc/LiCl), and the grafting of poly(lactic acid) onto microcrystalline cellulose by homogeneous ROP in ionic liquid [Bmim]Cl (Guo, Wang, Li, et al., 2012; Guo, Wang, Shu, Shen, & Sun, 2012). It was interesting to find that the amphiphilic cellulose derivatives were able to form self-assembled nanomicelles with diameters ranging between 10 and 100 nm, and were suitable to be applied as antitumor drug delivery vehicles (Guo, Wang, Li, et al., 2012) or fluorescent sensing carriers (Wang et al., 2012).

Poly(ε-caprolactone) (PCL) is a hydrophobic aliphatic polyester with excellent biodegradability, biocompatibility, low immunogenicity, nontoxicity, good mechanical and thermoplastic properties. PCL has been frequently applied as implantable biomedical materials and sustainable bionanocomposites (Habibi et al., 2008; Labet & Thielemans, 2011; Paquet, Krouit, Bras, Thielemans, & Belgacem, 2010). Block copolymers composing PCL as the hydrophobic part have also been intensively investigated as micelle-forming materials (Cai, Vijayan, Cheng, Lima, & Discher, 2007; Chang et al., 2008; Kim et al., 2006; Li et al., 2010), although grafted brush copolymer based on PCL and biomass has never been considered. It is promising to combine cellulose with the biodegradable polyester to produce amphiphilic copolymer and nanomicelles applicable to drug delivery and sensing systems.

In this study, novel biodegradable amphiphilic cellulose derivatives were prepared by grafting PCL onto underivatized cellulose via homogeneous ROP in ionic liquid [Bmim]Cl. The molecular architecture of the copolymers was controlled by selecting different catalyst, reaction temperature, cellulose:ε-CL feed ratio, etc. The resultant copolymers were thoroughly characterized by FT-IR, ^{1}H NMR, ^{13}C NMR, XRD, thermal analysis. The self-assembly of the cellulose-*g*-PCL copolymers were performed in water to obtain nanomicelles with PCL inner core and cellulose outer layer. The effect of molecular architecture on the self-assembly behavior of cellulose-*g*-PCL copolymers was discussed. Such cellulose-based biodegradable amphiphiles developed directly from biomass raw materials have a great potential of application as drug carriers and nanocarriers for diagnosis and sensing agents.

2. Experimental

2.1. Materials

The cellulose substrate, softwood dissolved pulp (degree of polymerization: 750) was purchased from Shandong bohi industry Co., Ltd., and was used after being washed with deionized water, milled, and vacuum dried at 65 °C for 48 h. The ionic liquids (IL) 1-N-butyl-3-methylimidazolium chloride ([Bmim]Cl) with a purity of 99.0% (Cheng Jie Chemical Co., Ltd., Shanghai, China) were dried in vacuum for 48 h at 45 °C before use. The monomer ε-caprolactone (CL) with a purity of 99.5% and stannous octanoate ($Sn(Oct)_2$) were purchased from Aladdin-reagent Inc. and were used as received without any further purification. 4-Dimethylaminoptridine (DMAP) with a purity of 99.0% was provided by Saen Chemical Technic Co., Ltd. Pyrene of 99.9% purity was provided by Sigma Chemical. All the other solvents were of analytical reagent grade and directly used without further purification.

2.2. Synthesis of cellulose-g-PCL copolymers

Cellulose (0.3 g) was added to 10 g [Bmim]Cl in a 25 mL dried three-neck flask. The mixture was vigorously stirred at 80 °C for 2 h with the protection of nitrogen to make a homogeneous solution. Then the monomer of ε-CL and 0.2 wt.% $Sn(Oct)_2$ or DMAP as the catalyst were slowly added into the solution, and the ring opening graft polymerization was carried out at 100 °C or 130 °C under nitrogen atmosphere with vigorous stirring for 24 h. After cooling to room temperature, the resultant copolymer was isolated by precipitating the reaction mixture into 250 mL ethanol and washed for several times. Subsequently, the copolymer was suspended in dichloromethane and magnetically stirred at room temperature for 48 h to dissolve homo-PCL, which could be formed during the grafting reaction. Finally, the copolymers was filtered through a glass filter (0.45 μm) and washed several times with more dichloromethane in order to confirm the absence of any free homo-polymer. The final product was dried in vacuum for 48 h at 60 °C.

2.3. Characterization of cellulose-g-PCL copolymers

The FT-IR spectra of cellulose-*g*-PCL copolymers were collected from a Bruker spectrometer (TENSOR27, Switzerland) in KBr discs. The ^{1}H NMR and ^{13}C NMR spectra were recorded on a Bruker AV-III 400 M spectrometer (Germany) using DMSO-d_6 as solvents. The chemical shifts were calibrated against the internal standard signals of tramethysilane (TMS). X-ray diffraction (XRD) was determined by a D/max-IIIA X-ray diffractometer, in which the high-intensity monochromatic nickel-filtered Cu Kα radiation was generated at 40 kV and 40 mA. Samples were scanned at a speed of 1°/min and a step size of 0.04° in the range of $2\theta = 5–70°$ at room temperature. The thermal stability of the cellulose-*g*-PCL copolymers was analyzed by a thermogravimetric analysis (TGA) (TGA Q500, TA, USA). Samples of approximately 10 mg weight were heated in an aluminum crucible to 600 °C at a heating rate of 10 °C/min while the apparatus was continually flushed with a nitrogen flow of 30 mL min^{-1}.

The solubility of the obtained graft copolymers in water and DMSO, respectively, was tested by the method as following: The sample was dispersed in solvent (water or DMSO) at a concentration of 10 mg/mL and followed by magnetic stirring at room temperature for 24 h. Then the solutions were visually observed. The samples with no visible precipitation were regarded as soluble. The samples with expanded volume in the solution were treated as swell, while those with no evidence of swelling were regarded as undissolving.

2.4. Preparation of cellulose-g-PCL self-assembled micelles

In a typical experiment, 20 mg cellulose-*g*-PCL copolymer was dissolved in 1 mL DMSO. The solution was slowly dropped into 5 mL ultrapure water under vigorous stirring. Then the solution was dialyzed against plenty of deionized water for 24 h (refresh the deionized water every 6 h) in a dialysis bag with MWCO = 3000 Dalton. After the DMSO was completely removed, the dialyzed solutions were adjusted to a definite concentration for subsequent analysis.

2.5. Dynamic light scattering (DLS)

The hydrodynamic size and size distribution (PDI) of polymeric micelles in water were determined by dynamic light scattering (DLS). Measurements were carried out at 25 °C using Zetasizer 3000 HS instrument at 90° scattering angle with a 633 nm He–Ne laser

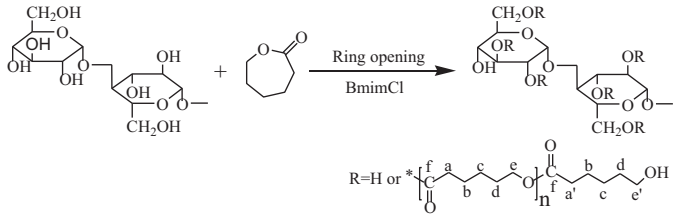

Scheme 1. The grafting copolymerization of PCL onto cellulose backbone in ionic liquid [Bmim]Cl.

using backscattering detection. All analyses were run for five times, and the results were recorded as the average values.

2.6. Scanning electron microscopy (SEM) analysis

SEM sample was prepared by casting a droplet of dilute polymeric micelles solutions onto a mica sheet and then dried at room temperature. After gold-plating, the sample was observed on a field emission scanning electron microscopy (LEO 1530 VP, LEO, Germany).

2.7. Determination of critical micelle concentration (CMC)

The CMC values of cellulose-*g*-PCL copolymers were determined by using pyrene as the hydrophobic probe with fluorescence spectroscopy (Jobin-Yvon Fluorolog Tau-3 system, American). Polymeric micelle solutions (10 mL) of various concentrations (0.0035–2 mg/mL) were prepared by dialysis method. A known amount of pyrene tetrahydrofuran (THF) solution (6×10^{-5} M) was added to each pre-prepared micelle solution, and then the THF was removed with a flow of nitrogen. The final concentration of pyrene in micelle solution was controlled to be 6×10^{-7} M. The sample solutions were then sonicated for 30 min at room temperature to equilibrate pyrene. Fluorescence spectra were measured at the excitation wavelength of 339 nm, and the emission spectra were collected in the range of 360–550 nm. The excitation and emission slit widths were set at 10.0 and 2.5 nm, respectively. Based on the pyrene emission spectra, the emission intensity ratio of I_{375}/I_{386} was plotted against the log concentration of cellulose-*g*-PCL copolymers. The CMC values were calculated based on the crossover point whereas I_{375}/I_{386} began to decrease rapidly.

3. Results and discussion

3.1. Synthesis of cellulose-g-PCL

A series of PCL grafted cellulose brush copolymers were synthesized via homogeneous ROP of ε-CL onto cellulose in ionic liquid [Bmim]Cl. Scheme 1 illustrates the route of the synthesis of cellulose-*g*-PCL copolymers. Soft wood dissolved pulp with high content of cellulose (98%) was chosen as the reaction substrate, and ionic liquid [Bmim]Cl, a powerful solvent for biomass, was employed to make the ROP reaction performed in a homogeneous environment. In order to adjust the hydrophilic/hydrophobic balance of the graft copolymers, the feed ratio of cellulose with ε-CL was varied ([AGU]/[CL] = 1:6–1:20, Table 1). As a result, the degree of substitution (DS) of PCL in the resultant copolymers is varied in a wide range (0.09–2.41). Moreover, the effects of the catalyst type and reaction temperature on the extent of grafting were investigated.

ROP of lactones is most commonly performed in the presence of metal-based catalyst (e.g. $Sn(Oct)_2$) (Habibi et al., 2008; Yuan, Yuan, Zhang, & Xie, 2007). Recently, organic catalysts (e.g. N,N-dimethylamino-4-pyridine (DMAP) and citric acid) with more availability and selectivity begin to be applied in ε-CL polymerization (Coulembier, Degee, Hedrick, & Dubois, 2006; Labet & Thielemans, 2012). To compare the catalytic effect of traditional metal-based catalyst and new organic catalyst in the grafting copolymerization of cellulose with ε-CL, two typical catalyst ($Sn(Oct)_2$, DMAP) were studied in parallel. It turned out that DMAP was a more powerful catalyst for the ROP of ε-CL onto cellulose in ionic liquid. According to the results of Table 1, with all the other conditions kept same, the copolymers synthesized using DMAP as catalyst show significantly higher grafting amount of PCL (in terms of MS, DS, W_{PCL}) than those synthesized using $Sn(Oct)_2$ as catalyst. A possible reason for this phenomenon is the stereochemistry of ε-CL. Both of the two catalysts do not require additional co-initiator or activated precursor to catalyze the ROP of ε-CL onto cellulose, whereas the hydroxyl groups of cellulose play important roles as the initiators. In the $Sn(Oct)_2$ catalyzed ROP reaction, the catalyst is firstly attached to cellulose hydroxyl groups via trans-alcoholysis reaction, and then ROP of ε-CL is initiated by coordination insertion of the catalyst on the monomer followed by the propagation step. The ROP of ε-CL in presence of DMAP takes place by the nucleophilic attack of the initially activated hydroxyl groups of cellulose on the carbonyl carbon. The puckered stereochemistry of ε-CL is more favorable to the nucleophilic attach than the coordination insertion (Coulembier et al., 2006; Labet & Thielemans, 2012), thus DMAP shows higher catalytic activity in this case.

The higher reaction temperature was found to be favor to the graft copolymerization of cellulose with ε-CL. According to the results of Table 1, the reactions performed at 130 °C resulted in higher grafting ratios than those performed at 100 °C. All of the copolymers synthesized at 130 °C were able to be dissolved in DMSO due to the higher grafting ratio. However, the water solubility of the cellulose-*g*-PCL copolymers was not as good as that of the cellulose-*g*-PLA copolymers (Guo, Wang, Shu, et al., 2012) probably due to the crystalline properties of PCL segments (Kusumi, Teramoto, & Nishio, 2008). The samples prepared at 100 °C in presence of $Sn(Oct)_2$ with low ε-CL in feed ratio (less than 15 molar times of AGU) had limited solubilities either in organic solvent or in water due to the low graft amount. As a result, the exact PCL grafting amount of them cannot be analyzed by NMR.

3.2. Characterization of cellulose-g-PCL

The FT-IR spectra of unmodified cellulose substrate and the cellulose-*g*-PCL copolymers with varying grafting ratios are displayed in Fig. 1. The bands at 2933 cm^{-1} and 2860 cm^{-1} (C—H stretching of —CH_3 and —CH_2— groups), 1732 cm^{-1} (carbonyl group), and 1144 cm^{-1} (C—H bending) present in the spectra of the grafted samples but absent in their unmodified precursors (Dong et al., 2008; Xu, Kenneay, & Liu, 2008). Moreover, the intensity of these signals was enhanced obviously as the grafting amounts of PCL increase. In order to confirm these signals are originated from the PCL grafted onto cellulose but not from the homo-PCL mixed with cellulose, a sample of regenerated cellulose (Reg-cellulose) was prepared by mixing dissolved pulp and ε-CL in [Bmim]Cl at 130 °C for 8 h followed by the removal of homo-PCL by dichloromethane extraction. The FT-IR spectrum of Reg-cellulose indicated that ungrafted homo-PCL could be completed removed, and the signals were solely contributed by the grafted PCL chains.

The typical ^{13}C NMR spectrum of cellulose-*g*-PCL copolymer (CGCL5) is shown in Fig. 2A. The carbonyl carbon signal of the PCL segment (in the *f* position) is at δ = 173.1 ppm. The methylene carbon signals of PCL can be observed at δ = 32.0 ppm, 33.7 ppm, 25.1 ppm, 24.1 ppm, 27.7 ppm, 60.3 ppm and 63.5 ppm corresponding to the carbons in the *a*, *a*′, *b*, *c*, *d*, *e*′ and *e* positions, respectively. At the same time, the carbons of the cellulose backbone appear

Table 1
Reaction conditions and properties of cellulose-*g*-PCL copolymers.

Samples	[AGU]/[CL]	Catalysts (wt%)	T (°C)	DP_{PCL}[a]	MS[b]	DS[c]	W_{PCL} (%)[d]	Solubilities	
								DMSO	H_2O
CGCL1	1:6	2% $Sn(oct)_2$	130	2.29	0.20	0.09	12.34	+++	–
CGCL2	1:8	2% $Sn(oct)_2$	130	2.47	0.42	0.17	20.00	+++	–
CGCL3	1:10	2% $Sn(oct)_2$	130	2.88	0.68	0.24	32.36	+++	–
CGCL4	1:15	2% $Sn(oct)_2$	130	2.62	1.07	0.41	42.95	+++	–
CGCL5	1:20	2% $Sn(oct)_2$	130	2.92	2.89	0.99	67.04	+++	–
CGCL6	1:15	2% $Sn(oct)_2$	100	–	–	–	–	+	–
CGCL7	1:15	2% DMAP	100	2.89	3.22	1.11	74.69	+++	–
CGCL8	1:15	2% DMAP	130	2.84	5.31	1.87	78.89	+++	–
CGCL9	1:20	2% DMAP	130	3.05	7.35	2.41	83.80	+++	–

+++: dissolving; +: swelling; –: undissolving.
[a] The degree of polymerization of PCL, calculated by ^{1}H NMR: $DP = (I_a + I_{a'})/I_{a'}$.
[b] Molar composition in graft copolymer, calculated by ^{1}H NMR: $MS = (I_a + I_{a'})/2H_4$.
[c] The degree of substitution of copolymer, calculated by ^{1}H NMR: $DS = I_{a'}/2H_4$.
[d] The content of PCL, calculated by ^{1}H NMR: $W_{PCL} = 100MS \times 114/(162+MS \times 114)$.

at δ = 102.0 ppm, 80.6 ppm, 70.0–76.9 ppm, and 63.5 ppm assigned to the C_1, C_4, $C_{2,3,5}$, and C_6 in the anhydrous glucose units (AGU), respectively (Yan, Zhang, et al., 2009). Moreover, the signal corresponding to the overlap of C_6 bearing substituted —OH group with the methylene carbon of PCL in the *e*′ position appears at δ = 60.3 ppm. The carbon signal at δ = 99.5 ppm belongs to the C_1 adjacent to the C_2 with substituted —OH groups, indicating PCL grafts at multiple sites of AGU.

In the ^{1}H NMR spectrum of cellulose-*g*-PCL copolymer (CGCL5) (Fig. 2B), the methylene proton peaks of PCL can be observed at δ = 4.0 ppm (—CH_2O—, *e*, repeating units), 3.37 ppm (—CH_2OH, *e*′, end unit), 2.26 ppm (—$COCH_2$—, *a*′, end unit), 1.53 ppm (—$COCH_2$—, *a*, repeating unit), 1.40 ppm (—CH_2—, *b*, *d*), and 1.30 ppm (—CH_2—, *c*) (Jiang et al., 2011). The resonance peaks derived from the protons of AGU of cellulose backbone appear at δ = 4.65 ppm, 3.78 ppm, 3.57 ppm, 3.05 ppm attributed by H_1, H_3, $H_{5,6,2}$, H_4, respectively. Meanwhile, the signals at δ = 5.51 ppm, 5.37 ppm, and 4.32 ppm correspond to the protons of the residual hydroxyl groups of AGU. According to these assignments, the molecular factors of the graft copolymers including DP, MS, DS and weight content of PCL side

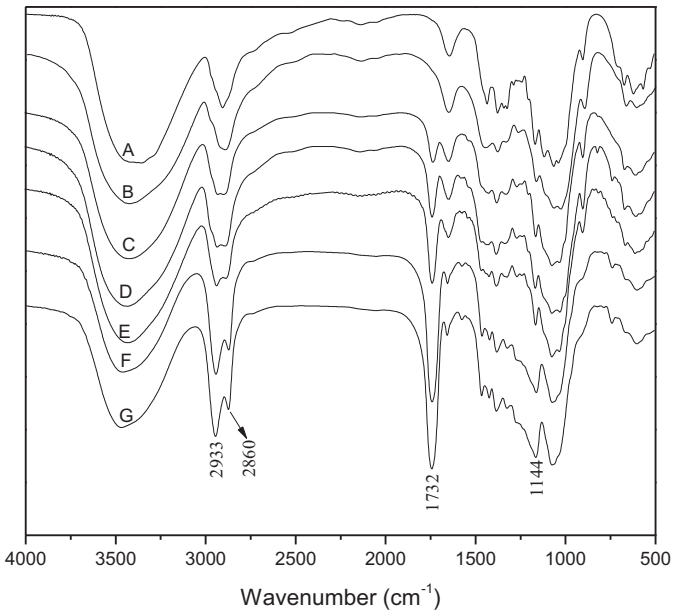

Fig. 1. The FT-IR spectra of dissolved cellulose and cellulose-*g*-PCL copolymers (A: cellulose; B: Reg-cellulose; C: CGCL3; D: CGCL4; E: CGCL5; F: CGCL8; G: CGCL9).

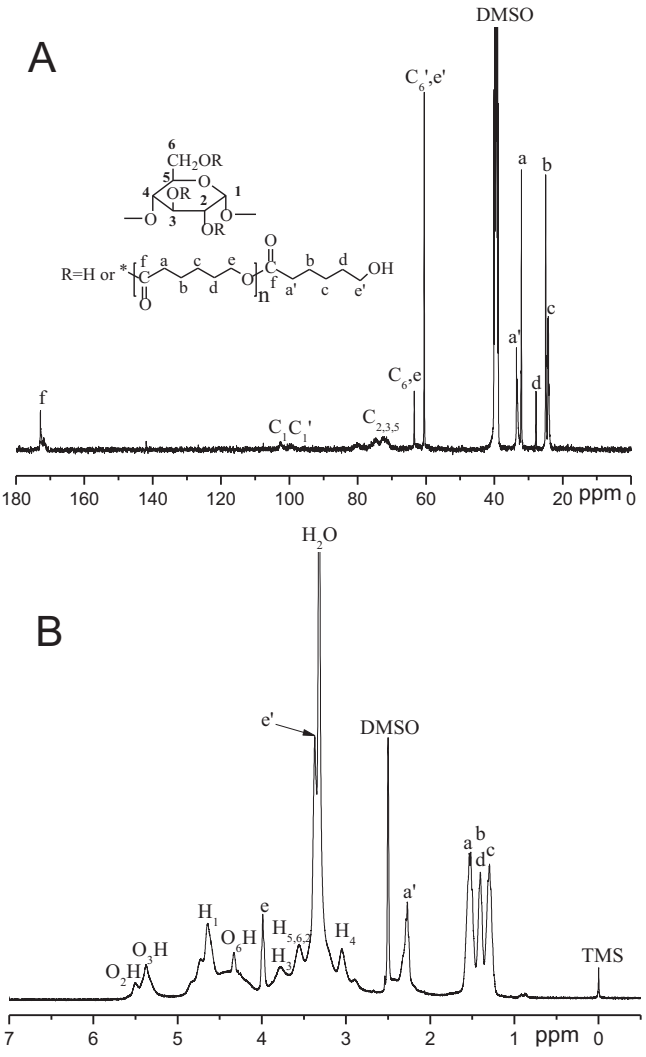

Fig. 2. The typical ^{13}C NMR (a) and ^{1}H NMR (b) spectrum of cellulose-*g*-PCL copolymers (CGCL5).

chains were estimated by the calculations with the peak intensity of corresponding signals based on the following equations:

$$MS = \frac{CL}{AGU} = \frac{I_{(a+a')}/2}{I_{H_4}} \quad (1)$$

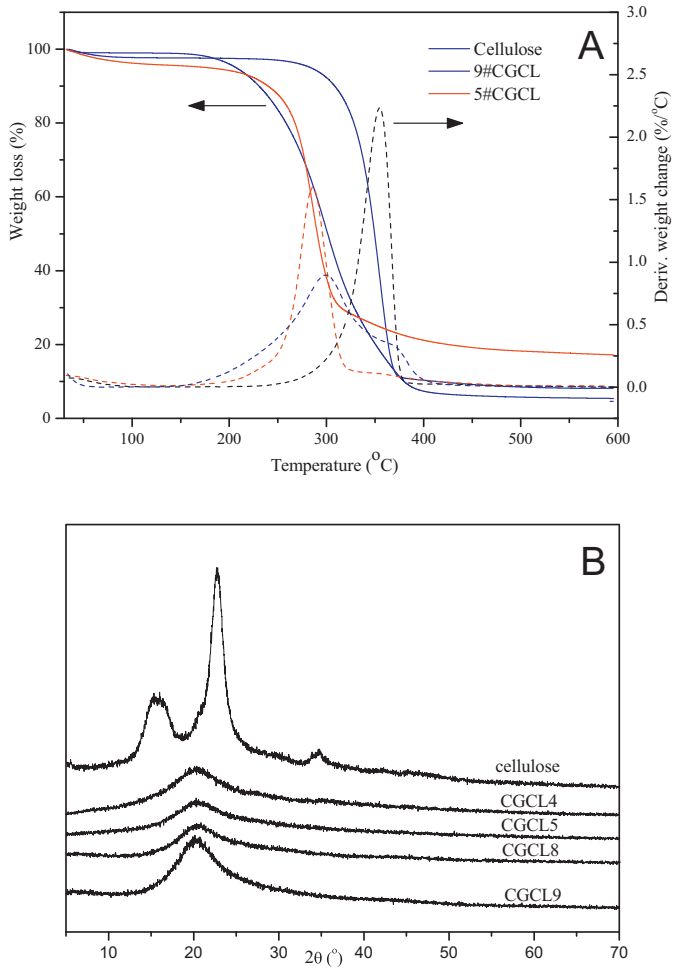

Fig. 3. The TGA (a) and XRD (b) spectra of cellulose and cellulose-*g*-PCL copolymers.

$$DS = \frac{\text{terminal CL}}{\text{AGU}} = \frac{I_{a'}/2}{I_{H_4}} \quad (2)$$

$$DP_{PCL} = \frac{MS}{DS} = \frac{I_a}{I_{a'}} + 1 \quad (3)$$

$$W_{PCL} = \frac{114MS}{162 + 114MS} \times 100\% \quad (4)$$

where MS is the molar substitution of PCL, DS is the degree of substitution of PCL (e.g. the number of PCL side chains per cellulose unit), DP_{PCL} is the degree of polymerization of PCL and W_{PCL} is the weight content of PCL side chains. The 114 g mol^{-1} and 162 g mol^{-1} in Eq. (4) are the molecular weight of ε-CL monomer and the molecular weight of cellulose repeating unit, respectively. The calculated structural factors for the cellulose-*g*-PCL copolymers are presented in Table 1.

The thermal stabilities of cellulose and cellulose-*g*-PCL copolymers with different grafting ratios (CGCL5, CGCL9) in nitrogen were determined by thermal gravimetric analysis (Fig. 3A). The TG curve of pure cellulose shows single stage decomposition with the onset of weight loss at about 255 °C. For CGCL5 and CGCL9, the weight loss starts at lower temperature at about 214 °C and 163 °C, respectively. There were two overlapped broad peaks could be observed in the DTG curve of CGCL9. The first decomposition peak may be attributed to the degradation of cellulose, and the second one should be due to the decomposition of PCL side chains. In the DTG curve of CGCL5, the decomposition peak of cellulose could be found easily while the decomposition peak corresponding to the scission of PCL is hardly observed due to the small grafting amount of PCL in CGCL5. In general, the initial decomposition temperature and maximum thermal degradation temperature (T_{max}) of cellulose-*g*-PCL copolymers were lower than those of free cellulose, indicating the thermal stability is reduced after grafting PCL. This phenomenon could be explained by the reduction of hydrogen bonds and change in the crystalline structure of cellulose backbone after introducing PCL side chains.

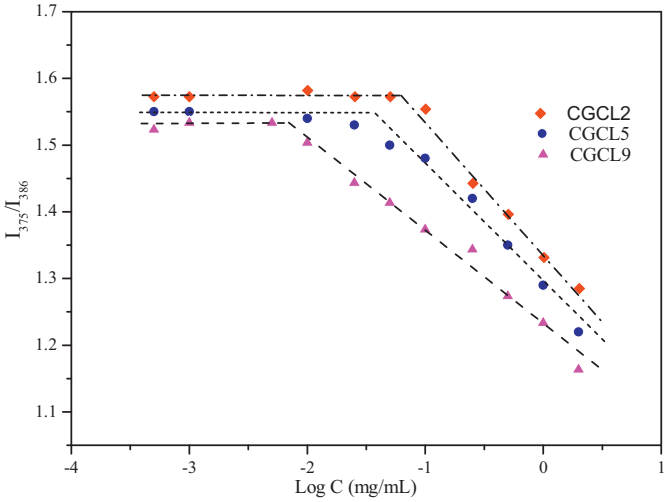

Fig. 4. Plots of the I_1/I_3 ratio of pyrene emission spectra in water as a function of the log concentration of cellulose-*g*-PCL copolymers.

Fig. 3B shows the XRD patterns of cellulose and cellulose-*g*-PCL copolymers with various PCL contents. The XRD pattern of cellulose shows a semi-crystalline character with well-defined diffraction peaks located at $2\theta = 15.90°$, 22.76°, and 34.86°, corresponding to the diffraction planes of (1 0 1), (0 0 2), and (0 4 0), respectively (Park, Baker, Himmel, Parilla, & Johnson, 2010). None of the above peaks could be observed in the diffraction patterns of cellulose-*g*-PCL copolymers, suggesting that the original crystalline structure of cellulose had been disrupted by the introduction of PCL side chains. This is consistent with the results from the TGA analysis. On the other hand, a new wide peak centered at $2\theta = 21.4°$ corresponding to the (1 1 0) plane of PCL chains appeared in the diffraction patterns of copolymers (Kim et al., 2006), and the intensity of which increased with growing DS of PCL. This suggested that the PCL segments in cellulose-*g*-PCL copolymers existed mainly in a crystalline state, and the longer chains facilitated the formation of ordered crystalline arrangement.

3.3. *Self-assembly of cellulose-g-PCL in water*

The self-assembly process of cellulose-*g*-PCL was triggered by a drop-wise addition of the copolymer's DMSO solution into water under stirring, and then followed by the slow exchange of organic solvent DMSO against water through a dialysis process. Dialysis of copolymer solution has the advantage of complete removal of the solvent under ambient conditions. The self-assembled cellulose-*g*-PCL nanoparticles consisted of PCL cores were surrounded by cellulose coronas. The particle size and size distribution (polydispersity, PDI) of the resulting nanoparticles self-assembled in water were demonstrated by dynamic light scattering (DLS) techniques and the results were displayed in Table 2. The average hydrodynamic radiuses (R_h) of cellulose-*g*-PCL nanoparticles with different PCL contents were mostly below 100 nm. All the nanoparticles exhibited unimodal size distribution. Interestingly, smaller particles could be observed with increasing content of PCL in the copolymers. When the DS of PCL was increased from 0.09 to 2.41, the average particle size was reduced from about 100 nm to near

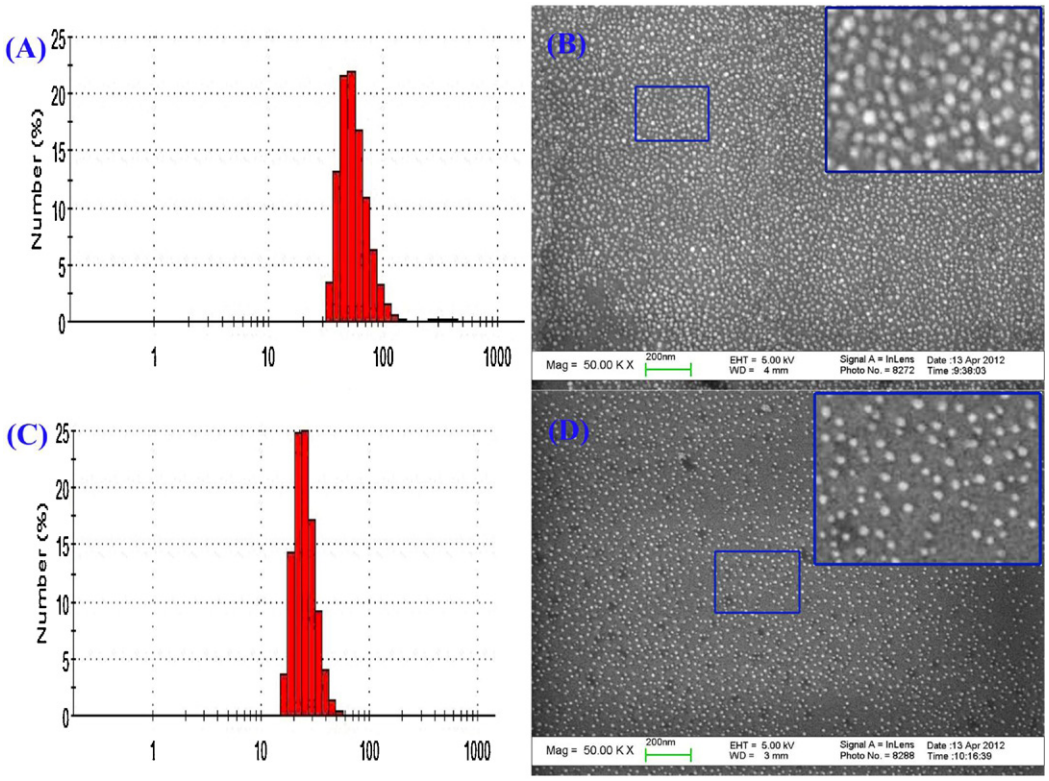

Fig. 5. The size histogram of cellulose-*g*-PCL micelles (CGCL5: A; CGCL9: C) determined by DLS and their SEM images (CGCL5: B; CGCL9: D).

20 nm. This may be due to that the hydrophobic PCL chain length of the cellulose-*g*-PCL copolymers obtained in this study is slightly changed with increasing DS of PCL. As a result, increasing content of hydrophobic segments in the copolymers would not lead to expanded volume, but result in stronger hydrophobic interaction and more compact core structure.

The self-assembly behavior of cellulose-*g*-PCL copolymers were studied by a fluorescent probe method. A hydrophobic florescent dye pyrene was chosen as the fluorescent probe. Pyrene is very sensitive to the polarity changes in the microenvironment (Aguiar, Carpena, Molina-Bolivar, & Ruiz, 2003). When the micelles are formed in water solution, pyrene molecules preferentially partition in the hydrophobic microdomains, and at the same time the molecule's photophysical properties would exhibit significant changes. The intensity ratio of the first fluorescence emission peak (375 nm, I_1) to the third emission peak (386 nm, I_3) of pyrene is usually used as the indicator of the polarity of the pyrene environment. Fig. 4 shows the emission intensity ratio of I_1/I_3 of pyrene as a function of the logarithm concentration of cellulose-*g*-PCL copolymers in water. It could be seen that the intensity ratio of I_1/I_3 kept briefly constant at low concentration of copolymers, and then had a linear decrease as the concentration reaches a limit value. The limit concentration is the critical micelle concentration (CMC) of the amphiphilic copolymer, which is the threshold concentration of self-assembled micelles formation. Low CMC value indicates a strong tendency toward formation of micelles in aqueous solution and a better stability against dilution. According to the plot curves of the cellulose-*g*-PCL copolymers with high DS of PCL (CGCL9), medium DS of PCL (CGCL5) and low DS of PCL (CGCL2) in Fig. 4, it can be deduced that higher hydrophobicity of the copolymer leads to stronger micelle forming ability in water. Detailed CMC values of the cellulose-*g*-PCL copolymers with various PCL content determined by fluorescence assay are summarized in Table 2.

Table 2
Results from characterization of cellulose-*g*-PCL micelles in aqueous solution.

Samples	CMC (μg/mL)	Hydrodynamic radiuses (R_h) (nm)	Polydispersity (PDI)
CGCL1	78.80	98.2 ± 13.9	0.419 ± 0.055
CGCL2	62.81	102.00 ± 11.91	0.325 ± 0.018
CGCL3	44.07	87.67 ± 2.68	0.407 ± 0.032
CGCL4	41.12	71.76 ± 4.02	0.370 ± 0.018
CGCL5	37.53	48.70 ± 0.26	0.378 ± 0.005
CGCL8	7.51	25.55 ± 1.01	0.261 ± 0.012
CGCL9	5.86	18.81 ± 1.41	0.300 ± 0.042

The morphology of the cellulose-*g*-PCL nanomicelles was observed by SEM, as depicted in Fig. 5B and D. It can be seen that the particles are uniformly distributed with well-defined spherical structures. The observed micelle size of CGCL5 (about 50 nm) was obviously larger than that of CGCL9 (about 20 nm). This was consistent with the results of DLS analysis. The corresponding size distribution diagrams of CGCL5 and CGCL9 are displayed in Fig. 5A and C, confirming that the obtained nanomicelles have narrow size distributions.

4. Conclusions

A series of biodegradable amphiphilic cellulose-*g*-PCL copolymers with varying molecular factors were synthesized via homogeneous ROP of ε-CL onto underivatized cellulose backbone in ionic liquid [Bmim]Cl. The successive synthesis was confirmed by FT-IR, ^{1}H NMR, ^{13}C NMR analysis. The obtained copolymers showed significantly different solubilities, crystalline structures and thermal properties from their precursor. The self-assembly behaviors of these copolymers in water and their nanomicelles were characterized by fluorescence spectrum, DLS and SEM. The results showed that the CMC values and micelles sizes were relevant with molecular structure of the cellulose-*g*-PCL copolymers. With the DS of PCL increased from 0.09 to 2.41, the CMC and micelle sizes of the copolymers varied in the range of 5.86–78.80 μg/mL

and 18.81–102.00 nm, respectively. It is noteworthy that the novel amphiphilic copolymers from biomass are completely composed of biodegradable, renewable materials. They should have a great potential for applications in biomedicine and nanotechnology.

Acknowledgements

The authors gratefully acknowledge the financial support from the National Science Foundation of China (No. 51103046) and the Ministry of Science and Technology of China (973 project, No. 2010CB732201 and 2010CB732204).

References

Aguiar, J., Carpena, P., Molina-Bolivar, J. A., & Ruiz, C. C. (2003). On the determination of the critical micelle concentration by the pyrene 1:3 ratio method. *Journal of Colloid and Interface Science*, *258*(1), 116–122.

Cai, S., Vijayan, K., Cheng, D., Lima, E. M., & Discher, D. E. (2007). Micelles of different morphologies – Advantages of worm-like filomicelles of PEO–PCL in paclitaxel delivery. *Pharmaceutical Research*, *24*(11), 2099–2109.

Carlmark, A., & Malmstrom, E. (2003). ATRP grafting from cellulose fibers to create block-copolymer grafts. *Biomacromolecules*, *4*(6), 1740–1745.

Chang, C., Peng, J., Zhang, L., & Pang, D.-W. (2009). Strongly fluorescent hydrogels with quantum dots embedded in cellulose matrices. *Journal of Materials Chemistry*, *19*(41), 7771–7776.

Chang, C., Wei, H., Quan, C.-Y., Li, Y.-Y., Liu, J., Wang, Z.-C., et al. (2008). Fabrication of thermosensitive PCL–PNIPAAm–PCL triblock copolymeric micelles for drug delivery. *Journal of Polymer Science Part A: Polymer Chemistry*, *46*(9), 3048–3057.

Chao-Hsuan, C., Nguyen-Van, C., Yung-Tsung, C., So, R. C., Liau, I., & Ming-Fa, H. (2011). Overcoming multidrug resistance of breast cancer cells by the micellar doxorubicin nanoparticles of mPEG–PCL-graft-cellulose. *Journal of Nanoscience and Nanotechnology*, *11*(1).

Coulembier, O., Degee, P., Hedrick, J., & Dubois, P. (2006). From controlled ring-opening polymerization to biodegradable aliphatic polyester: Especially poly(beta-malic acid) derivatives. *Progress in Polymer Science*, *31*(8), 723–747.

Dong, H., Xu, Q., Li, Y., Mo, S., Cai, S., & Liu, L. (2008). The synthesis of biodegradable graft copolymer cellulose-graft-poly(L-lactide) and the study of its controlled drug release. *Colloids and Surfaces B: Biointerfaces*, *66*(1), 26–33.

Dou, H., Jiang, M., Peng, H., Chen, D., & Hong, Y. (2003). pH-dependent self-assembly: Micellization and micelle-hollow-sphere transition of cellulose-based copolymers. *Angewandte Chemie: International Edition*, *42*(13), 1516–1519.

Francis, M. F., Piredda, M., & Winnik, F. M. (2003). Solubilization of poorly water soluble drugs in micelles of hydrophobically modified hydroxypropylcellulose copolymers. *Journal of Controlled Release*, *93*(1), 59–68.

Guo, Y., Wang, X., Li, D., Du, H., Wang, X., & Sun, R. (2012). Synthesis and characterization of hydrophobic long-chain fatty acylated cellulose and its self-assembled nanoparticles. *Polymer Bulletin*, *69*(4), 389–403.

Guo, Y., Wang, X., Shu, X., Shen, Z., & Sun, R. (2012). Self-assembly and paclitaxel loading capacity of cellulose-graft-poly(lactide) nanomicelles. *Journal of Agricultural and Food Chemistry*, *60*(15), 3900–3908.

Habibi, Y., & Dufresne, A. (2008). Highly filled bionanocomposites from functionalized polysaccharide nanocrystals. *Biomacromolecules*, *9*(7), 1974–1980.

Habibi, Y., Goffin, A.-L., Schiltz, N., Duquesne, E., Dubois, P., & Dufresne, A. (2008). Bionanocomposites based on poly(epsilon-caprolactone)-grafted cellulose nanocrystals by ring-opening polymerization. *Journal of Materials Chemistry*, *18*(41), 5002–5010.

Hassani, L. N., Hendra, F., & Bouchemal, K. (2012). Auto-associative amphiphilic polysaccharides as drug delivery systems. *Drug Discovery Today*, *17*(11–12), 608–614.

Hsieh, M.-F., Van Cuong, N., Chen, C.-H., Chen, Y. T., & Yeh, J.-M. (2008). Nano-sized micelles of block copolymers of methoxy poly(ethylene glycol)-poly(epsilon-caprolactone)-graft-2-hydroxyethyl cellulose for doxorubicin delivery. *Journal of Nanoscience and Nanotechnology*, *8*(5), 2362–2368.

Jiang, C., Wang, X., Sun, P., & Yang, C. (2011). Synthesis and solution behavior of poly(epsilon-caprolactone) grafted hydroxyethyl cellulose copolymers. *International Journal of Biological Macromolecules*, *48*(1), 210–214.

Kang, H., Liu, W., He, B., Shen, D., Ma, L., & Huang, Y. (2006). Synthesis of amphiphilic ethyl cellulose grafting poly(acrylic acid) copolymers and their self-assembly morphologies in water. *Polymer*, *47*(23), 7927–7934.

Kim, M. S., Hyun, H., Seo, K. S., Cho, Y. H., Lee, J. W., Lee, C. R., et al. (2006). Preparation and characterization of MPEG–PCL diblock copolymers with thermo-responsive sol–gel–sol phase transition. *Journal of Polymer Science Part A: Polymer Chemistry*, *44*(18), 5413–5423.

Krouit, M., Bras, J., & Belgacem, M. N. (2008). Cellulose surface grafting with polycaprolactone by heterogeneous click-chemistry. *European Polymer Journal*, *44*(12), 4074–4081.

Kusumi, R., Teramoto, Y., & Nishio, Y. (2008). Crystallization behavior of poly(epsilon-caprolactone) grafted onto cellulose alkyl esters: Effects of copolymer composition miscibility. *Macromolecular Chemistry and Physics*, *209*(20), 2135–2146.

Labet, M., & Thielemans, W. (2011). Improving the reproducibility of chemical reactions on the surface of cellulose nanocrystals: ROP of epsilon-caprolactone as a case study. *Cellulose*, *18*(3), 607–617.

Labet, M., & Thielemans, W. (2012). Citric acid as a benign alternative to metal catalysts for the production of cellulose-grafted-polycaprolactone copolymers. *Polymer Chemistry*, *3*(3), 679–684.

Li, X., Kong, X., Shi, S., Wang, X., Gu, Y., Guo, G., et al. (2010). Preparation, characterization, and self-assembly behavior of a novel MPEG/PCL-g-chitosan copolymer. *Soft Materials*, *8*(4), 320–337.

Li, Y., Liu, R., Liu, W., Kang, H., Wu, M., & Huang, Y. (2008). Synthesis, self-assembly, and thermosensitive properties of ethyl cellulose-g-P(PEGMA) amphiphilic copolymers. *Journal of Polymer Science Part A: Polymer Chemistry*, *46*(20), 6907–6915.

Liu, W., Liu, Y., Hao, X., Zeng, G., Wang, W., Liu, R., et al. (2012). Backbone-collapsed intra- and inter-molecular self-assembly of cellulose-based dense graft copolymer. *Carbohydrate Polymers*, *88*(1), 290–298.

Liu, X., Chen, J., Sun, P., Liu, Z.-W., & Liu, Z.-T. (2010). Grafting modification of ramie fibers with poly(2,2,2-trifluoroethyl methacrylate) via reversible addition-fragmentation chain transfer (RAFT) polymerization in supercritical carbon dioxide. *Reactive & Functional Polymers*, *70*(12), 972–979.

Lonnberg, H., Fogelstrom, L., Berglund, M. A. S. A. S. L., Malmstrom, E., & Hult, A. (2008). Surface grafting of microfibrillated cellulose with poly(epsilon-caprolactone) – Synthesis and characterization. *European Polymer Journal*, *44*(9), 2991–2997.

Ostmark, E., Nystrom, D., & Malmstrom, E. (2008). Unimolecular nanocontainers prepared by ROP and subsequent ATRP from hydroxypropylcellulose. *Macromolecules*, *41*(12), 4405–4415.

Paquet, O., Krouit, M., Bras, J., Thielemans, W., & Belgacem, M. N. (2010). Surface modification of cellulose by PCL grafts. *Acta Materialia*, *58*(3), 792–801.

Park, S., Baker, J. O., Himmel, M. E., Parilla, P. A., & Johnson, D. K. (2010). Cellulose crystallinity index: Measurement techniques and their impact on interpreting cellulase performance. *Biotechnology for Biofuels*, *3*, 10.

Roy, D., Semsarilar, M., Guthrie, J. T., & Perrier, S. (2009). Cellulose modification by polymer grafting: A review. *Chemical Society Reviews*, *38*(7), 2046–2064.

Song, Y., Zhang, L., Gan, W., Zhou, J., & Zhang, L. (2011). Self-assembled micelles based on hydrophobically modified quaternized cellulose for drug delivery. *Colloids and Surfaces B: Biointerfaces*, *83*(2), 313–320.

Sui, X., Yuan, J., Zhou, M., Zhang, J., Yang, H., Yuan, W., et al. (2008). Synthesis of cellulose-graft-poly(N,N-dimethylamino-2-ethyl methacrylate) copolymers via homogeneous ATRP and their aggregates in aqueous media. *Biomacromolecules*, *9*(10), 2615–2620.

Wan, S., Jiang, M., & Zhang, G. (2007). Dual temperature- and pH-dependent self-assembly of cellulose-based copolymer with a pair of complementary grafts. *Macromolecules*, *40*(15), 5552–5558.

Wang, D., Tan, J., Kang, H., Ma, L., Jin, X., Liu, R., et al. (2011). Synthesis, self-assembly and drug release behaviors of pH-responsive copolymers ethyl cellulose-graft-PDEAEMA through ATRP. *Carbohydrate Polymers*, *84*(1), 195–202.

Wang, X., Guo, Y., Li, D., Chen, H., & Sun, R. (2012). Fluorescent amphiphilic cellulose nanoaggregates for sensing trace explosives in aqueous solution. *Chemical Communications*, *48*(45), 5569–5571.

Wang, X., & Sun, R. (2011). Self-assembled lignocellulose micelles: A new generation of value-added functional nanostructures. *Bioresources*, *6*(3), 2288–2290.

Wei, Y., Cheng, F., Hou, G., & Sun, S. (2008). Amphiphilic cellulose: Surface activity and aqueous self-assembly into nano-sized polymeric micelles. *Reactive & Functional Polymers*, *68*(5), 981–989.

Xu, Q., Kenneay, J., & Liu, L. (2008). An ionic liquid as reaction media in the ring opening graft polymerization of epsilon-caprolactone onto starch granules. *Carohydrate Polymers*, *72*, 113–121.

Yan, Q., Yuan, J., Zhang, F., Sui, X., Xie, X., Yin, Y., et al. (2009). Cellulose-based dual graft molecular brushes as potential drug nanocarriers: Stimulus-responsive micelles, self-assembled phase transition behavior, and tunable crystalline morphologies. *Biomacromolecules*, *10*(8), 2033–2042.

Yan, C., Zhang, J., Lv, Y., Yu, J., Wu, J., Zhang, J., et al. (2009). Thermoplastic cellulose-graft-poly(L-lactide) copolymers homogeneously synthesized in an ionic liquid with 4-dimethylaminopyridine catalyst. *Biomacromolecules*, *10*(8), 2013–2018.

Yuan, W., Yuan, J., Zhang, F., & Xie, X. (2007). Syntheses, characterization, and in vitro degradation of ethyl cellulose-graft-poly(epsilon-caprolactone)-block-poly(L-lactide) copolymers by sequential ring-opening polymerization. *Biomacromolecules*, *8*(4), 1101–1108.

Yuan, W., Zhang, J., Zou, H., Shen, T., & Ren, J. (2012). Amphiphilic ethyl cellulose brush polymers with mono and dual side chains: Facile synthesis, self-assembly, and tunable temperature–pH responsivities. *Polymer*, *53*(4), 956–966.